Edan Khan[1], Bodduru Kamesh[1]*, Mesfin Kebede Kassa[2,3], Iqra Javid[4]

[1]*Department of Mechanical Engineering, Sharda University, Greater Noida, India,* [2]*Department of Mechanical Engineering, Kombolcha Institute of Technology, Wollo University, Kombolcha, Ethiopia,* [3]*School of Aerospace Engineering, Ethiopian Aviation University, Ethiopian Airlines, Addis Ababa, Ethiopia.* [4]*Department of Electrical, electronics, and Communication Engineering, Sharda University, Greater Noida, India.*

Mechanical properties investigation of hybrid Tl$_3$C$_2$T$_X$ MXene and carbon nanotube reinforced glass fiber epoxy composites

ABSTRACT

The current work, presents the synergistic effects of carbon nanotubes (CNTs) and MXene nanoplatelets (MXN) on the flexural, hardness, and water absorption properties of laminated glass fiber reinforced polymer (GFRP) composites. The composites specimens with various concentrations of CNTs and MXN were fabricated by cost-effective vacuum-assisted hand lay-up technique. The results showed that the hybrid composite reinforced with CNT and MXN improved the flexural strength and hardness by 38% and 29%, respectively. It was also observed that the hybrid composite reinforced with MXN and CNT exhibited superior mechanical and water absorption properties. Moreover, MXN/CNT reinforced GFRP hybrid composites exhibited a weight gain of 1.004%, while the neat epoxy-reinforced GFRP composite showed a higher weight gain at 1.210%. Further, the elastic characteristics of hybrid glass fiber-reinforced epoxy composite were found to be significantly affected by the addition of MXNs rather than CNTs.
Keywords: *MXene nanoplatelet, carbon nanotube, glass fiber, flexural property, water uptake capacity*

1. INTRODUCTION

Nowadays, there is a growing interest in Carbon nanotubes (CNTs) and MXene (MXN) based nanocomposites in various fields such as automotive, aerospace and aircraft industry due to their excellent properties including lightweight, high strength, and load-carrying capacity [1-3]. MXenes (MXN) are 2D structured flakes with a size of approximately 100nm. They have a Hexagonal Close Packing crystallographic structure which makes them well suited for adhesion with polymeric matrices. Their popularity is on the rise across various applications such as bio-sensors, ionic state batteries, and super-capacitors composites [4-7]. However, CNTs are three-dimensional tubular nanostructures with C-C bonds. These bonds provide CNTs with properties that make them beneficial when used in composite structures. Single-walled carbon nanotubes (SWCNTs) and multi-walled carbon nanotubes (MWCNTs), which

are comparatively inexpensive, are both available as rolled MXene sheets. Researchers are further exploring the mechanical properties of CNTs and MXN for strengthening various polymer composite materials, particularly epoxy resin composites. To mention a few, Verma et al. investigated the water absorption properties of jute fiber reinforced starch-glycerol biocomposites and showed that the epoxy resin layer can block the main disadvantage of the biocomposite, which leads to poor water absorption of the composites [8]. Varma et al. investigated the mechanical, thermal, and microstructural properties of epoxy-based human hair (HH) reinforced composites. The authors revealed that the optimal combination was a cured epoxy-based composite with a weight percentage based human hair fibre component [9]. Moreover, Lila et al. presented the variables influencing the impact strength of epoxy composites reinforced with synthetic fibres [10]. Rastogi et al. examined the nonwoven waste cellulose fabric reinforced epoxy-based composite's mechanical strength and thermal stability. The obtained results suggested that the composite produces a high degree of toughness and can be applied for coating purposes [11]. Additionally, the thermal and physical characteristics of an epoxy hybrid composite filled with a mixture of chicken feather fibre (CFF) and

Corresponding author: Bodduru Kamesh

E-mail: bodduru.kamesh@sharda.ac.in

crumb rubber (CR) with varying CFF and CR weight percentages were characterized.

Their research demonstrated that the hybrid composite's qualities were much better than those of the pure fiber-reinforced composite [12]. Wang et al. investigated the ultimate tensile strength and flexure properties of epoxy/carbon fiber composite laminates with various concentration of CNTs/GNPs hybrids [13]. Kamaraj et al. investigated the performance of laminated flax composites strengthened with different concentrations of MXN in terms of flexural, tensile, water absorption, and flammability. The authors revealed that the most favourable outcomes in tensile and flexural strength were achieved at a concentration of 0.1wt% of MXN [14]. Shen et al. examined the cryogenic interlaminar shear strength (ILSS) of glass fiber-reinforced polymer (GFRP) composites enhanced with GNP oxide (MO). The authors demonstrated that the incorporation of GNP reduced the likelihood of crack formation, thereby enhancing the laminate's resistance to fractures. Limited research has explored the use of MXene as nanofillers [15]. Mahmood et al. conducted a comprehensive experimental and numerical analysis to assess the influence of MXene on the bending behavior of GFR epoxy composites. The authors revealed that incorporating 0.3wt% MXene oxide (MO) increased the cryogenic interlaminar shear strength (ILSS) of GFRP composites by 32.1%. In addition, MO-coated laminated composites were also found to have superior mechanical properties compared to MO-reinforced laminated GFRP composites compared to uncoated laminated composites [16]. Civalek et al. studied the mechanical and thermal stability characteristics of multifunctional sandwich nanocomposites and showed that the introduction of different concentrations of MXN helps to improve the mechanical and thermal stability of the nanocomposites [17]. Chiang et al. investigated the mechanical properties carbon-fibre-reinforced polymer (CFRP) reinforced with hybridized CNT and MXene under diverse temperature conditions, encompassing moisture levels at 85°C,65°C, and 25°C. The obtained results showed that the incorporation of filler reinforcements resulted in improved mechanical properties of CFRP [18]. Qin et al. investigated the mechanical and interfacial characteristics of laminated CFRP composites reinforced with CNT and MXene nanoparticles. The authors reported that the addition of CNT and MXene fillers improved the tensile strength by 70% and flexural strength by 52% [19]. Wang et al. investigated the quasi-static and dynamic response of woven and unidirectional laminated CFRP metal with the addition of MXene nanoparticles [20]. Liu et al. experimentally studied the overall mechanical properties, thermal conductivity and fracture toughness of nanocomposites incorporating MXN and CNT and revealed that the experimental investigation is a challenging, expensive, and time-intensive endeavor [21].

Bottom of Form In addition, Verma et al. reviewed atomistic modeling methods for predicting fracture toughness, thermal conductivity, and mechanical properties of graphene/hexagonal boron nitride polymer nanocomposites and showed that atomistic modeling methods are cost-effective and time-saving compared to experimental methods [22]. Furthermore, Varma et al. illustrated the challenges associated with nanomechanics-based approach of water desalination [23]. Varma et al. performed a Molecular dynamics based atomistic simulations coupled with the reactive force field parameters to capture atomic interactions within graphene and polyethylene atoms and revealed that the strength and toughness of nanocomposite can be improved by increasing the number of adhesion points between the nanofiller and matrix [24]. Further experimental and numerical studies on the mechanical and structural properties of composites associated with nanofillers can be found in [25–30]. As can be seen from the above literature, further research is needed to fully exploit the superior mechanical properties of MXN and CNTs as reinforcement in FRP composites. Therefore, the present study investigates the synergistic effects of CNTs and MXN on the flexural, hardness, and water absorption properties of laminated GFRP composites.

2. EXPERIMENTAL PROCEDURE

2.1. Materials

Unidirectional E-glass fibers with grade 220 GSM and 0.2 mm thickness were purchased from CF Composites Pvt. Ltd, India was procured was used. The Mxene nano-flakes exhibiting a purity of 99% and comprising 10 layers were procured from intelligent materials PVT. Ltd, India. MWCNTs (99% purity, 10–20 nm average diameter, and 6 μm average length are commercially available from Shilpa Enterprises (India). The epoxy resin (LY 556) and hardener (HY 951) were procured from CF composites.

2.2 Fabrication of multiscale nanocomposite laminates

Firstly, the CNT/MXN nanoparticles with appropriate weight fractions were sonicated in the epoxy resin polymer matrix for 1-hour using ultrasonication in order to increase the dispersion of the nanoparticles in the polymer matrix. Then, CNT/MXN reinforced polymer nanocomposite was

refluxed with HY-951 hardener solution with the ratio of 10:1. Subsequently, the CNT/MXN reinforced GFRP nanocomposites were fabricated using vacuum vacuum-assisted hand layup technique. After lamination, samples were stored in vacuum bags to remove excess resin and air bubbles. Finally, the samples were left to cure at room temperature. Finally, per ASTM guidelines, the samples were precisely cut to the desired dimensions for each test.

3. EXPERIMENTAL TEST PROCEDURE

3.1 Flexural test

Three rectangular specimens of each composition with dimensions 60mm × 10mm × 6mm were cut from the fully cured samples for three-point, in compliance with ASTM D790 [31]. the test was conducted at room temperature. The universal testing machine (INNOTECH UTM, India) operated at a crosshead speed of 2 mm/min, and a maximum load capacity of 3000kg UTM was used for testing. The flexural strength, flexural modulus, and flexural strain were obtained by using the following expressions:

$$\sigma_f = \frac{3PL}{2bd^2} \tag{1}$$

$$E_f = \frac{L^3 M}{4bd^3} \tag{2}$$

$$\varepsilon_f = \frac{6Dd}{L^2} \tag{3}$$

where the symbol σ_f denotes the flexural strength, E_f denotes flexural modulus, and ε_f denotes flexural strain. Additionally, M represents the slope of the load-deflection curve, P represents maximum load, L represents the length of the support span, b represents breadth, D represents maximum deflection and d represents depth of the specimen.

3.2. Void content

In the present study, the void content of the nanocomposite specimens was obtained in accordance with ASTM D2734-94 [32]. Equation (4) was then employed to compute the theoretical density (ρ_{ct}).

$$\rho_{ct} = 1 \bigg/ \left(\frac{w_f}{\rho_f} + \frac{w_m}{\rho_m} + \frac{w_{CNT}}{\rho_{CNT}} + \frac{w_{MXN}}{\rho_{MXN}} \right) \tag{4}$$

where, w_f, w_m, w_{CNT}, and w_{MXN} represent the weight of the glass fiber, polymer matrix, CNTs,

and MXNs, respectively; ρ_f, ρ_m, ρ_{CNT}, and ρ_{GNP} represents the density of fiber, matrix, CNT, and MXN, respectively. Void content in the samples was determined by using the following equation:

$$V_V = \frac{\varrho_{ct} - \varrho_{ce}}{\varrho_{ct}} \times 100 \tag{5}$$

where V_V represents the void content (%) and ρ_c represents the experimental density.

3.3 Vickers hardness

A Rockwell Vickers hardness tester (INNOTECH UTM, India) was used for hardness testing. The preparation of the nanocomposite samples complied with ASTM D-2240 [33]. The indenter has a maximum load of 50 kg and a 1/16-inch diameter. The hardness measurements were made 15 seconds after the surface of the produced nanocomposite samples was in close contact with the diamond indenter. Each nanocomposite sample configuration underwent the application of a force of 490.5 N on its upper surface, and the hardness value was computed based on 10 recorded measurements. The determination of the hardness value employed in the subsequent equation:

$$HV = \frac{0.1891 \times F}{D^2} \tag{6}$$

where HV, F, and D represent the hardness value, the load of the indenter, and the diameter of the indenter, respectively.

3.4. Water absorption test

Three rectangular specimens of each composition with dimensions 10mm × 10mm × 3.5 mm were cut from the fully cured samples for water absorption test, in compliance with ASTM D570, and placed in a water bath at room temperature for about 75 days. At regular intervals, each sample was first removed from distilled water and dried off before weighting using weight balance. The water content (W) percentage was determined using the following equation:

$$W = \frac{W_t + W_i}{W} \times 100 \tag{7}$$

where W represents the percentage of water absorption; W_t and W_i denote the weight of the sample after immersion and before immersion in the water, respectively.

4. RESULTS AND DISCUSSION

4.1. Mechanical properties

The flexural properties of hybrid fiber-reinforced laminated composites with various nanofillers such

as CNT and MXN-reinforced GFRP composites are discussed in this section. It can be noticed from Figure 1 that a three-point bending test was performed to evaluate the load applied relative to deflection across different nanocomposite configurations.
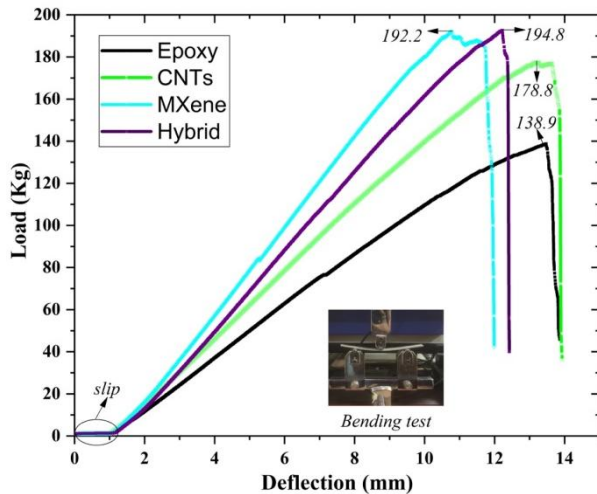

Figure 1. Load v/s deflection for various nanocomposite configurations.

The deflection rises proportionally with the applied load for all nanocomposite combinations, continuing until the test sample reaches its limit and can no longer bear additional loading. Additionally, the nanocomposite samples made of epoxy, CNTs, MXNs, and hybridized can bear higher loads than neat epoxy composite. It was shown that the hybrid composite demonstrates superior load-bearing capacity. This outcome could be attributed to the enhanced interfacial strength between the fibers and matrix, facilitated by both filler reinforcements, CNT and MXN.
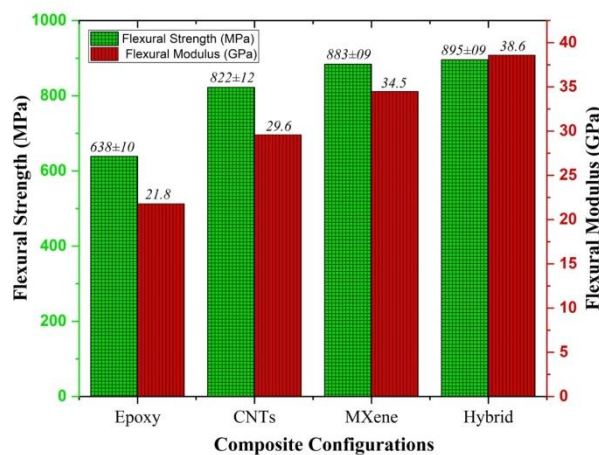

Figure 2. Flexural strength and flexural modulus of the fabricated specimens

Figure 2 illustrates the fluctuations in flexural strength and flexural modulus across different samples. The incorporation of nanoparticles enhances both flexural strength and flexural modulus. This effect may be attributed to the nanoparticles acting as slippage arresters within the layers of glass fiber and epoxy, mitigating crack propagation. Moreover, when a load is applied, tension may transfer from the epoxy to the MXN/CNT-reinforced nanoparticles. The hybrid GFRP nanoparticles exhibited a 38% increase in flexural strength compared to the neat epoxy composite. Conversely, the composite reinforced with MXN demonstrated the highest flexural modulus. This is because the elastic modulus of the MXN is substantially larger than that of the CNT. The assessment of flexural strength, flexural modulus and peak strain values for the mentioned entities supports the conclusion that the hybrid composite reinforced with CNT and MXN is most suitable for diverse applications. With regard to flexural strength, the hybrid composite, MXN-reinforced composite, CNT-reinforced composite, and neat epoxy all exhibited elevated hardness values. MXN gives the matrix a sizable contact area thanks to its large surface area. In contrast to CNTs, which only have exterior surfaces, MXNs have interaction with the matrix on both of their surfaces. Additionally, MXNs have a rougher nanoscale surface than MWCNTs, which allows for a stronger interlocking of the fiber/matrix contact. Figure 3 exhibits images of the failed sample for a better understanding of the fracture behavior. Upon comparing the sample of neat epoxy composite with that of the hybrid composite, it is obvious that the neat epoxy composite sample exhibits important delamination. In a clean epoxy composite, fiber breakage and distinct matrix separation are both visible.

Figure 3. Photographs illustrating the damage mechanism in (a) neat epoxy composite and (b) CNT/MXN reinforced hybrid composite sample

4.2. Microstructural characterization of fractured laminated composite

Scanning Electron Microscope (SEM) was used to investigate the microstructural features of the prepared hybrid laminated composites. It was observed that the MXene/CNTs reinforced composite prevented fiber breakage due to the presence of MXene/CNT nanofillers. Figure 4 (a, b) presents the raw powder of MXene and CNT, while (c) shows the breaking surface of the hybrid composite, and (d) illustrates the presence of

MXene/CNTs on the glass fiber composite. Notably, the fabricated composites display minimal defects and showcase robust adhesion between the matrix and reinforcements, as well as strong bonding between the fibers and MXene/CNT nanofillers.
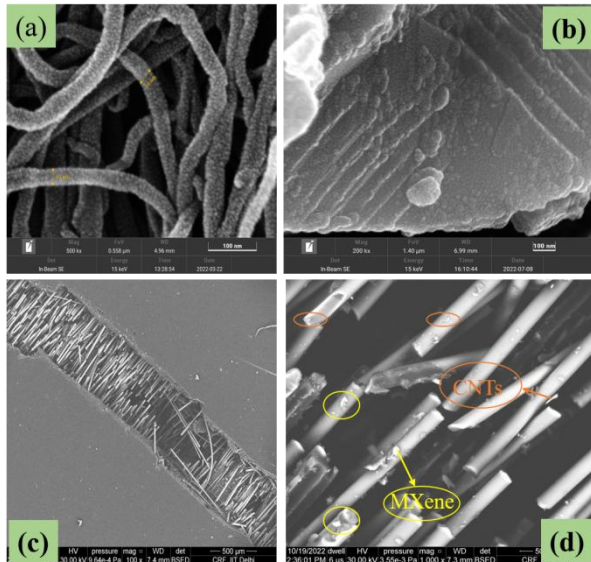

Figure 4. (a, b) SEM images of CNT and MXene nanofiller, (c) CNT/MXN reinforced hybrid composite fiber breaking phenomenon, and (d) the presence of MXN/CNTs over the glass fiber composite

4.3. Void content and density

It is widely accepted that trapped air volatilities occur in composites created utilizing the hand layup process when the matrix is impregnated into the fiber. The flow of resin through the fiber layer influences the distribution of voids during both the fabrication and curing processes, potentially affecting the mechanical and physical properties [42]. An expected consequence of voids is the anticipated degradation of the mechanical and physical properties of the composites. A comprehensive examination of the void content in the fabricated composite specimens is imperative. The values for theoretical density, measured density, and voids identified in the produced specimens are presented in Table 1.

The samples containing nanoparticles had relatively low void contents, in contrast to neat epoxy, which had a greater void percentage among the composite specimens under investigation. Although there was a hypothesis suggesting that the geometry and morphology of the filler material play a substantial role in void content, in this instance, samples containing nanoparticles exhibited comparable levels of void content. The formation of voids in the sample can be attributed to nanoparticle agglomeration, which indicates a relatively uniform dispersion of nanoparticles.

Table 1. Details of hardness, density, and voids present in the studied specimens

Sl. no.	Composite samples	Hardness (VHN)	Experimental density (g/cm^3)	Theoretical density (g/cm^3)	Void content (%)
1	Epoxy	148 ± 5	1.089	1.160	6.519
2	CNTs	168 ± 7	1.092	1.154	5.677
3	MXNs	178 ± 5	1.098	1.155	5.2053
4	Hybrid	192 ± 8	1.095	1.155	5.479

4.4. Water uptake capacity

Figure 5 and Table 2 it provide examples of the ability of the composite sample to absorb water for different reinforcing fillers. It was indicated that the samples followed a similar trend regardless of the composite design. The water intake first rises sharply, but after it reaches saturation, the uptake virtually becomes steady. Owing to the presence of residual bubbles and flaws in the composite samples, the initial water absorption value surpasses the anticipated level. Nevertheless, with an increase in immersion duration, a saturated phenomenon becomes evident. Table 2 presents the average water uptake capacity of the composite samples.

Table 2. Increase in weight following the water absorption test for the manufactured samples

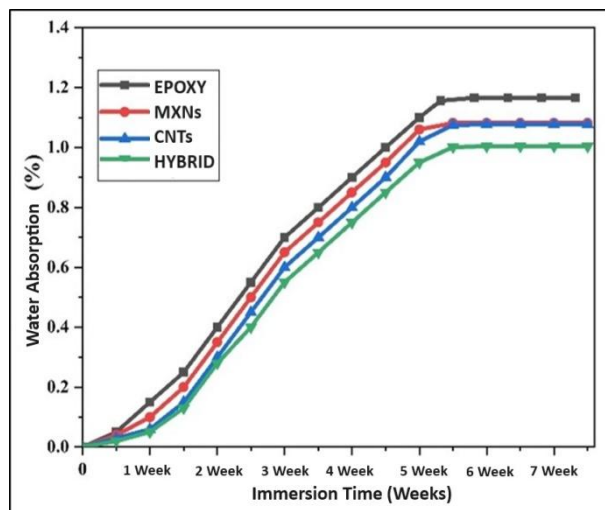| Sl. No.	Composite samples	The initial weight of the sample (Before immersion) (g)	The final weight of the sample (After immersion) (g)	Weight gain (%)
1	Epoxy	22.969	23.247	1.210
2	CNTs	25.622	25.899	1.081
3	MXNs	25.036	25.307	1.082
4	Hybrid	26.492	26.758	1.004

Figure 5. The changes in water absorption over time for the investigated samples

The glass fiber-reinforced composite sample with neat epoxy resin demonstrates the highest water uptake, while the hybrid composite reinforced with CNT and MXene exhibits the lowest water absorption value. Furthermore, among the examined materials, the order of water absorption, from highest to lowest, is observed in the neat epoxy, MXNs, CNTs, and hybrid samples. This demonstrates that the water barrier function of the nanofillers in GFRP composites lowers the absorption of water. This phenomenon is connected to the capability of nanofillers to restrict intermolecular accessibility within the surrounding GFRP composites, consequently delaying the relaxation of polymer chains and reducing the diffusion of small molecules through the composites. It is important to note that the water uptake capacity of GFRP composites varies depending on the specific type of nanofiller reinforcement used.

5. CONCLUSION

The present work investigated the synergetic influence of CNTs and MXene nanofillers on the flexural, hardness, water uptake, elasticity, and strength properties of GFRP composite. The composite with various concentrations of CNTs and MXN was fabricated by a cost-effective vacuum-assisted hand lay-up technique. The following key findings from his study are summarized as follows:

- The mechanical properties of the composite were enhanced through the addition of nanoparticles. The composite with this rein-forcement demonstrated superior mechanical characteristics compared to those with MXene and CNT individually. However, the hybrid GFRP composite containing both CNT and MXene displayed even higher flexural strength, and hardness was improved by 38% and 29%,

respectively, compared to the neat epoxy composite.
- The hybrid composite experienced a weight gain of 1.004%, while the neat epoxy composite exhibited a slightly higher weight gain of 1.210%. Notably, composites incorporating nanoparticles demonstrated enhanced water uptake capabilities. This improvement was described as the nanofiller's ability to restrict intermolecular mobility within the neighboring GFRP composites, thereby delaying the relaxation of polymer chains and reducing the diffusion of small molecules through the composites.
- The void percentage in the neat epoxy composite samples was the highest registering at 6.519%. Additionally, the vacancy content of nanoparticle-reinforced composite did not vary significantly. This could be explained by the nanoparticle's very uniform dispersion, as agglomeration causes void to appear in the sample.
- The impact of MXenes on the elastic properties of the hybrid glass-fiber reinforced epoxy nanocomposite is more significant compared to the influence of CNTs.
- The weight fraction exerts a notable influence on the aspect ratio of both CNTs and MXNs.

Conflict of Interest

The authors assert that there are no known competing financial interests or personal relationships that could have been perceived to influence the work reported in this paper.

Data Available Statement

The authors affirm that the data supporting the findings of this study can be found within the articles.

6. REFERENCES

[1] M.K.Kassa, A.B.Arumugam (2020) Micromechanical modeling and characterization of elastic behavior of carbon nanotube-reinforced polymer nano-composites: A combined numerical approach and experimental verification. Polym. Compos, 41(1), 3322-339. https://doi.org/10.1002/ pc.25622

[2] M. K.Kassa, A.B.Arumugam, T. Rana (2020) Three-phase modeling and characterization of elastic behavior of MWCNT reinforced GFRP composites: A combined numerical and experimental study. Materials Today: Proceedings, 26, 944-949. https://doi.org/10.1016/j.matpr.2020.01.152

[3] M.Kebede Kassa, A.B. Arumugam (2022) Bending response analysis of a laminated, tapered, curved, composite panel made from an agglomerated and wavy MWCNT–glass fiber–polymer hybrid. Transactions of the Canadian Society for Mechanical Engineering, 46(1), 103-131. https://doi.org/10.1016/j.matpr.2020.01.152

[4] A. Verma, A.Parashar (2017) The effect of STW defects on the mechanical properties and fracture toughness of pristine and hydrogenated graphene. Physical Chemistry Chemical Physics, 19(24), 16023-16037. https://doi.org/10.1039/C7CP02366A

[5] A.Verma, N.Jain, S.K.Sethi (2022) Modeling and simulation of MXene-based composites, in Innovations in MXene-Based Polymer Composites, Elsevier, pp. 167–198.

[6] A.Verma, A.Parashar (2018) Structural and chemical insights into thermal transport for strained functionalized graphene: a molecular dynamics study. Materials Research Express, 5 (11), 115605. https://doi.org/10.1088/2053-1591/aade36

[7] A.Verma, A.Gaur, V.K.Sing (2017) Mechanical properties and microstructure of starch and sisal fiber biocomposite modified with epoxy resin. Materials Performance and Characterization, 6(1), 500-520. https://doi.org/10.1520/MPC20170069

[8] A.Verma, K.Joshi, V.K.Singh (2018) Starch-jute fiber hybrid biocomposite modified with an epoxy resin coating: fabrication and experimental characterization. Journal of the Mechanical Behavior of Materials, 27(5-6), 20182006. https://doi.org/10.1515/jmbm-2018-2006

[9] A.Verma, V.K.Singh (2019) Mechanical, microstructural and thermal characterization of epoxy-based human hair–reinforced composites. Journal of Testing and Evaluation, (2), 1193-1215. https://doi.org/10.1520/JTE20170063

[10] M.K Lila, A.Verma, S.S.Bhurat (2022) Impact behaviors of epoxy/synthetic fiber composites. In Handbook of Epoxy/Fiber Composites Singapore: Springer Singapore (pp. 1-18). https://doi.org/10.1088/2053-1591/aaec28

[11] S.Rastogi, A.Verma, V.K.Singh (2020) Experimental response of nonwoven waste cellulose fabric–reinforced epoxy composites for high toughness and coating applications. Materials Performance and Characterization, 9(1), 151-172. https://doi.org/10.1520/MPC20190251

[12] A.Verma, P.Negi, V.K.Singh (2018) Physical and thermal characterization of chicken feather fiber and crumb rubber reformed epoxy resin hybrid composite. Advances in Civil Engineering Materials, 7(1), 538-55. https://doi.org/10.1520/ACEM20180027

[13] P.N.Wang, T. H.Hsieh, C.L.Chiang, M.Y.Shen (2015) Synergetic effects of mechanical properties on graphene nanoplatelet and multiwalled carbon nanotube hybrids reinforced epoxy/carbon fiber composites. Journal of Nanomaterials, 2015, 7-7. https://doi.org/10.1155/2015/838032

[14] M. Kamaraj, E.A. Dodson, S. Datta (2020) Effect of graphene on the properties of flax fabric reinforced epoxy composites. Advanced Composite Materials, 29(5), 443-458.
https://doi.org/10.1016/j.compositesb.2014.12.023

[15] X.J.Shen, L.X.Meng, Z.Y.Yan, C.J.Sun, Y.H.Ji, M. Xiao, S.Y.Fu (2015) Improved cryogenic interlaminar shear strength of glass fabric/epoxy composites by graphene oxide. Composites Part B: Engineering, 73, 126-131.
https://doi.org/10.1016/j.compositesb.2014.12.023

[16] H. Mahmood, L.Vanzetti, M.Bersani, A. Pegoretti (2018) Mechanical properties and strain monitoring of glass-epoxy composites with graphene-coated fibers. Composites Part A: Applied Science and Manufacturing, 107, 112-123. https://doi.org/10.1016/j.compositesa.2017.12.023

[17] Ö.Civalek, S.Dastjerdi, B.Akgöz (2022) Buckling and free vibrations of CNT-reinforced cross-ply laminated composite plates. *Mechanics Based Design of Structures and Machines*, *50*(6), 1914-1931. https://doi.org/10.1080/15397734.2020.1766494

[18] C.L. Chiang, H.Y.Chou, M.Y.Shen (2020) Effect of environmental aging on mechanical properties of graphene nanoplatelet/nanocarbon aerogel hybrid-reinforced epoxy/carbon fiber composite laminates. *Composites Part A: Applied Science and Manufacturing*, *130*, 105718.

https://doi.org/10.1016/j.compositesa.2019.105718

[19] W. Qin, C. Chen, J. Zhou, J. Meng (2020) Synergistic effects of graphene/carbon nanotubes hybrid coating on the interfacial and mechanical properties of fiber composites. *Materials*, *13*(6), 1457. https://doi.org/10.3390/ma13061457

[20] S. Wang, M. Cao, H. Xue, S. Araby, F. Abbassi, Y. He, Q. Meng (2022). Investigation on graphene addition on the quasi-static and dynamic responses of carbon fiber-reinforced metal laminates. *Thin-Walled Structures*, *174*, 109092.
https://doi.org/10.1016/j.tws.2022.109092

[21] J.Liu, J.Fu, T.Ni, Y.Yang (2019) Fracture toughness improvement of multi-wall carbon nanotu-bes/graphene sheets reinforced cement paste. *Construction and Building Materials*, *200*, 530-538. https://doi.org/10.1016/j.conbuildmat.2018.12.141l

[22] A.Verma, A.Parashar, M.Packirisamy (2018) Atomistic modeling of graphene/hexagonal boron nitride polymer nanocomposites: a review. *Wiley Interdisciplinary Reviews: Computational Molecular Science*, *8*(3), e1346.
https://doi.org/10.1002/wcms.1346

[23] A.Verma, A.Parashar, A.C.Van Duin (2022) Graphene-reinforced polymeric membranes for water desalination and gas separation/barrier applications. In *Innovations in Graphene-Based Polymer Composites* (pp. 133-165). Woodhead Publishing. https://doi.org/10.1016/B978-0-12-823789-2.00009-1

[24] A. Verma, A. Parashar, M. Packirisamy (2019) Effect of grain boundaries on the interfacial behavior of graphene-polyethylene nanocomposite. *Applied Surface Science*, *470*, 1085-1092. https://doi.org/10.1016/j.apsusc.2018.11.218

[25] M.K Kassa, R. Selvaraj, H. D. Wube, A. B. Arumugam (2023) Investigation of the bending response of carbon nanotubes reinforced laminated tapered spherical composite panels with the influence of waviness, interphase, and agglomeration. *Mechanics Based Design of Structures and Machines*, *51*(10), 5902-5924. https://doi.org/10.1080/15397734.2021.2017966

[26] M.K.Kassa, L.K.Singh, A.B.Arumugam (2022) Numerical and experimental investigation of first ply failure response of multi-walled carbon nanotubes/epoxy/glass fiber hybrid laminated tapered curved composite panels. Proceedings of the Institution of Mechanical Engineers, Part C: Journal of Mechanical Engineering Science. https://doi.org/10.1177/09544062221085896

[27] M.K.Kassa, A.B.Arumugam, B.Singh (2020) Prediction of Thermo-Mechanical Properties of MWCNT-Reinforced GFRP and Its Thermo-Elastic Response Analysis in Laminated Composite Plate. In *Proceedings of International Conference in Mechanical and Energy Technology: ICMET 2019, India* (pp. 285-296). Springer Singapore.

[28] M.Kishore, M.Amrita, B. Kamesh (2021) Tribological properties of basalt-jute hybrid composite with graphene as nanofiller. *Materials Today: Proceedings*, *43*, 244-249. https://doi.org/ 10.1016/j.matpr.2020.11.654

[29] M.Kishore, M.Amrita, B.Kamesh (2021) Experimental investigation of milling on basalt-jute hybrid composites with graphene as nanofiller. *Materials Today: Proceedings*, *43*, 726-730.

[30] M.K.Kassa, R.Selvaraj, H.D.Wube, A.B. Arumugam (2023) Investigation of the bending response of carbon nanotubes reinforced laminated tapered spherical composite panels with the influence of waviness, interphase, and agglomeration. *Mechanics Based Design of Structures and Machines*, *51*(10), 5902-5924. https://doi.org/10.1080/15397734.2021.2017966

[31] ASTM, S. (1997) Standard test methods for flexural properties of unreinforced and reinforced plastics and electrical insulating materials. ASTM D790. *Annual book of ASTM Standards*.

[32] ASTM D2734-94 (1994) Standard test methods for void content of reinforced plastics.

[33] ASTM D2240-15 (2021) Standard Test Method for Rubber Property- Durometer Hardness. doi: 10.1520/D2240-15R21.

IZVOD

SINERGETSKI EFEKAT MXene, CNT I HIBRIDNIH NANOČESTICA NA MEHANIČKA SVOJSTVA EPOKSIDNIH KOMPOZITA OJACANIH STAKLENIM VLAKNIMA

Sadašnji rad, predstavlja sinergističke efekte ugljeničnih nanocevi (CNT) i MXene nanopločica (MXN) na savijanje, tvrdoću i svojstva upijanja vode laminiranih polimernih kompozita ojačanih staklenim vlaknima (GFRP). Uzorci kompozita sa različitim koncentracijama CNT-a i MXN-a proizvedeni su ekonomičnom tehnikom ručnog polaganja uz pomoć vakuuma. Rezultati su pokazali da je hibridni kompozit ojačan CNT i MXN poboljšao čvrstoću na savijanje i tvrdoću za 38%, odnosno 29%. Takođe je primećeno da hibridni kompozit ojačan MXN i CNT pokazuje superiorna mehanička svojstva i svojstva upijanja vode. Štaviše, MXN/CNT ojačani GFRP hibridni kompoziti su pokazali povećanje težine od 1,004%, dok je čisti GFRP kompozit ojačan epoksidom pokazao veći porast težine od 1,210%. Dalje, utvrđeno je da na elastične karakteristike hibridnog epoksidnog kompozita ojačanog staklenim vlaknima značajno utiče dodavanje MXN, a ne CNT.
Ključne reči: *MXene nanoplocice, ugljenične nanocevi, stakleno vlakno, savijanje, kapacitet upijanja vode*

Bodduru Kamesh: https://orcid.org/0000-0001-6335-0815
Mesfin Kebede Kassa: https://orcid.org/0000-0002-1908-2769